International Journal of Machine Tools & Manufacture 51 (2011) 77–83

Contents lists available at ScienceDirect

International Journal of Machine Tools & Manufacture

journal homepage: www.elsevier.com/locate/ijmactool

Gap control for near-dry EDM milling with lead angle

Masahiro Fujiki [a], Gap-Yong Kim [b,*], Jun Ni [a], Albert J. Shih [a]

[a] Mechanical Engineering, University of Michigan, Ann Arbor, MI 48109-2125, USA
[b] Mechanical Engineering, Iowa State University, Ames, IA 50011-2161, USA

ARTICLE INFO

Article history:
Received 24 May 2010
Received in revised form
31 August 2010
Accepted 3 September 2010
Available online 18 September 2010

Keywords:
Electrical discharge machining
Gap control
Milling
Electrode

ABSTRACT

A new gap control strategy for five-axis milling using near-dry electrical discharge machining (EDM) has been experimentally investigated. The conventional EDM control strategy only allows the retraction of the electrode in the direction of machining trajectory, which results in inefficient gap control when the electrode is not perpendicular to the workpiece. The new gap controller is capable of retracting the electrode in the direction of its orientation. This enables more efficient enlargement of the discharge gap leading to faster recovery of average gap voltage. Experimental results show a 30% increase in material removal rate while the tool electrode wear ratio and surface roughness are not affected. Furthermore, EDM efficiency is improved due to the change in the electrode retraction in its axial direction. The gain tuning of the proposed controller is also discussed. This study shows the direction of electrode retraction is important for five-axis near-dry EDM milling.

1. Introduction

Electric discharge machining (EDM) is an electro-thermal process. When a large electric potential difference develops in the dielectric medium between electrically conductive electrode and the workpiece, the breakdown of dielectric medium creates a channel of plasma and melts the work-material for machining [1]. A reasonable amount of material removal is possible by controlling the electric potential difference between the workpiece and electrode at high frequency to maintain appropriate gap distance and condition. EDM milling [2] uses a rotating tubular electrode, which contours along a path, to create complex geometries on parts made from difficult-to-machine work-materials. The key advantage of EDM milling is that it does not require multiple electrodes. The geometry of electrode tip stays virtually unchanged during the machining process and tool electrode wear can be compensated in one dimension [3]. Research in dry EDM using gas as dielectric has been studied by Kunieda et al. [4–9] under the EDM milling configuration. Due to the reattachment of debris to the machined surface, dry EDM milling may have limitations to meet the combined material removal rate (MRR) and surface roughness requirements. This problem can be overcome in near-dry EDM by replacing the gas with the mixture of gas and dielectric liquid [10]. In addition, near-dry EDM milling does not require a bath of dielectric fluid, but only a small amount of dielectric fluid is sprayed around the machining area.

The control of EDM process is different from conventional machining process [11]. An additional gap control loop besides the servo control loop is needed in the EDM control. The average voltage during discharge, gap voltage (u_e), is constantly monitored, and the feed rate is overridden based on the difference between the reference gap voltage (u_{eref}) and monitored u_e. Therefore, the feed rate is constantly changing in EDM. Much work has been done to determine the output value of the manual feed rate override (MFO) function. Chang [12] developed a variable structure system (VSS) to enhance the robustness of the gap distance control. Zhang et al. [13] developed an adaptive fuzzy controller for the gap distance control. Kao et al. [14,15] also developed fuzzy controller using piezo stage for micro EDM hole drilling. Currently, research in gap control based on fuzzy control is becoming more popular since it utilizes the know-how of skilled operators [16]. However, the drawback of fuzzy controller is that it only controls the feed rate. To maximize the MRR for five-axis near-dry EDM milling, controlling methods beyond feed rate override is required. This is important because conventional feed rate override does not account for relative orientation of electrode and workpiece surface, and therefore, cannot efficiently enlarge the discharge gap for five-axis near-dry EDM milling.

Use of local actuator to enhance the flow of dielectric medium in the discharge gap has proven to improve the MRR in EDM processes by several researchers. Ultrasonic vibration can enhance the dielectric fluid flow in the discharge gap [17]. Nonetheless, ultrasonic vibration did not change the key discharge profiles, such as ignition time delay and average discharge energy, but decreased the number of short circuit and arcing. As a result, ultrasonic vibration improved the overall efficiency of machining process by 27%. Other studies showed that ultrasonic vibration increased MRR [18–21]. In dry EDM, however, it increased the tool electrode wear

* Corresponding author. Tel.: +515 294 6938; fax: +515 294 3261.
E-mail address: gykim@iastate.edu (G.-Y. Kim).

0890-6955/$ - see front matter © 2010 Elsevier Ltd. All rights reserved.
doi:10.1016/j.ijmachtools.2010.09.002

ratio and surface roughness [22–24]. One problem with ultrasonic vibration is that it does not optimize the mist flow rate through the discharge region, which is critical in near-dry EDM milling [25]. High bandwidth electrode positioning has also been investigated to enhance the MRR. A piezo actuator attached on an electrode can improve the MRR in EDM micro-hole drilling [26]. Further extension of the study has been made using electro-magnets [27]. A system that can position a small electrode in a three-dimensional space with high bandwidth has also been developed [28]. In dry EDM milling, a piezo actuator is attached beneath the workpiece and improvements in MRR and tool electrode wear ratio were observed [29]. Much work has been done in the control of EDM, but adequate investigations have lack of control strategies to improve the mist flow and MRR in five-axis near-dry EDM milling. Depending on the electrode orientation, the mist flow rate through the main discharge region (MDR) changes [25].

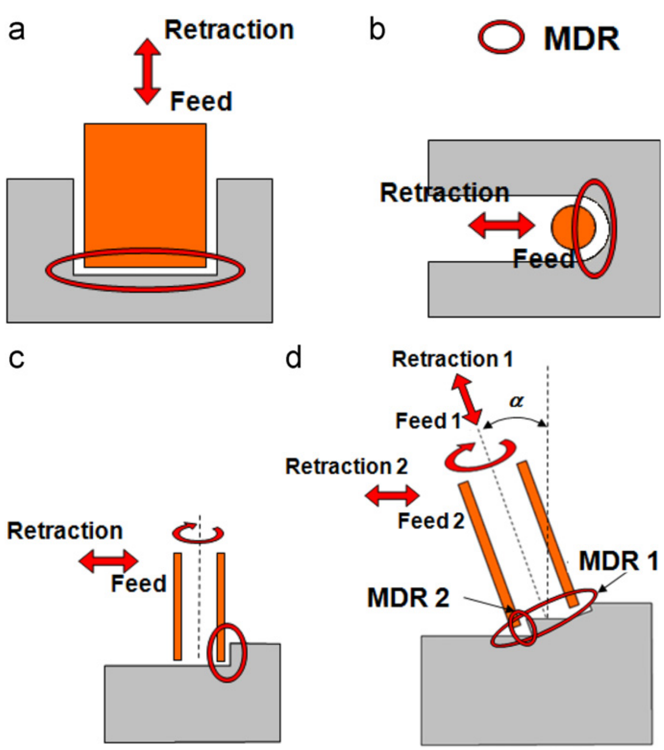

Fig. 1. Gap control and MDR in EDM: (a) sinking EDM, (b) wire EDM, (c) three-axis EDM milling, and (d) five-axis near-dry EDM milling.

This study investigates the use of a high-speed piezoelectric actuator to control the gap condition in near-dry EDM milling. A new control strategy specialized for near-dry EDM milling with lead angle using a piezoelectric actuator for gap condition control is developed. Experimental setup to investigate the control strategy is described. Detailed structure of a spindle system that retracts the electrode at high bandwidth is also discussed. Finally, experimental results on machining performance (MRR, tool electrode wear ratio, and surface roughness) using the proposed strategy are discussed, analyzed, and compared with the traditional gap control methods.

2. Gap control strategy for high-speed electrode retraction

In conventional EDM, machine is controlled by retracting electrode along a commanded trajectory based on the gap voltage regardless of type of EDM process. The feed and retract direction for sinking EDM, wire EDM, and three-axis EDM milling are illustrated in Fig. 1(a)–(c), respectively. This gap control strategy is adequate for these EDM configurations since the direction of retraction is always orthogonal to the MDR. The electrode retraction direction being orthogonal to the main discharge plane maximizes the efficiency of gap enlargement, which then leads to better debris flushing. For five-axis EDM milling, retracting the electrode along the trajectory is not efficient because the MDR is typically not orthogonal to the retract direction. Fig. 1(d) shows two MDR regions, denoted as MDR 1 and MDR 2, in the EDM milling with lead angle. MDR 1 is located at the bottom tip of electrode, and MDR 2 is located at the inner trailing face of electrode. To efficiently enlarge the gap distance, the electrode should retract in the direction of the electrode orientation, in the direction of retraction 1 as shown in Fig. 1(d), rather than in the direction of retraction 2. In this study, a novel method to control the gap by moving the electrode in both direction of feed/retraction 1 and 2, as shown in Fig. 1(d), in near-dry EDM is investigated.

A control structure that separates the electrode retraction and electrode feed along the path is the key to the proposed control strategy. The feed rate override function cannot be implemented to the near-dry EDM milling with lead angle (Fig. 1(d)) since the feed direction and the electrode retraction direction do not align. Fig. 2 shows the block diagram of the proposed control algorithm. The movement of electrode is separated into two parts, one is the motion along the planned trajectory (*XYZ* axes), and the other is the auxiliary axis motion, which is defined as the movement of the electrode along the direction of electrode orientation. Two controllers exist in the proposed architecture. The proposed

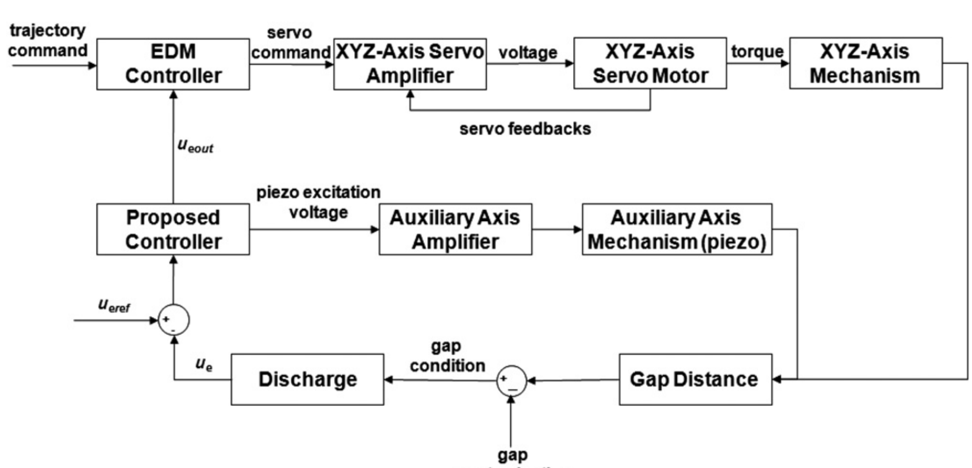

Fig. 2. Block diagram of proposed controller.

controller controls the position of auxiliary axis driven by a piezo actuator based on the difference between the reference gap voltage, u_{eref}, and the average gap voltage feedback, u_e. The proposed controller also regulates the motion of X, Y, and Z axes by outputting modified average gap voltage, u_{eout}, to the EDM controller. The EDM controller changes the feed rate based on the difference between u_{eout} and u_{eref}. The EDM controller moves the electrode forward along the trajectory when the difference is positive and retracts the electrode when the difference is negative. The motion of X, Y, Z and auxiliary axis changes the gap distance to maintain stable discharges.

Fig. 3 shows the flowchart of the proposed control algorithm. Two control modes exist in the proposed controller, the first being the trajectory mode in which the electrode moves forward along the planned trajectory. The second is the auxiliary axis mode in which electrode moves in its orientation direction. The controller switches back and forth between these two modes based on a status of a parameter, M. When the mode M is 0, the controller runs in the trajectory mode; when M switches to 1, the controller runs in the auxiliary axis mode in the next sampling time. The opposite configuration also occurs in the opposite position.

The proposed controller has three inputs and three outputs. The three inputs are M, gap voltage from the machine (u_e), and position of auxiliary axis (P_{aux}). Likewise, the three outputs are M, gap voltage output to the EDM machine's controller (u_{eout}), and incremental position command to the auxiliary axis (P_{com}). At the beginning of the servo loop, the controller checks the value of M to decide which control mode it will run. At the end of each control loop, the proposed controller updates the value of M based on P_{aux} and u_e. These two parameters prevent the cross talk between the two modes. Detailed algorithm of each control mode is discussed in the following section.

2.1. Trajectory mode ($M=0$)

The controller first checks the difference between the reference gap voltage, u_{eref}, and the gap voltage from the machine, u_e. If the voltage differential is positive, the controller maintains M at 0, outputs u_e to the EDM machine's main controller, and sets P_{com} to 0. The output runs the controller in trajectory mode in the next sampling time, and moves the electrode along the trajectory while maintaining the auxiliary axis to the current position.

When the voltage difference is negative, the controller changes M–1, outputs u_{eref} to the EDM machine's main controller, and sets P_{com} as the following:

$$P_{com}=K_R(u_{eref}-u_e) \tag{1}$$

where K_R is the constant gain in proportional control for retracting. The output runs the controller in the auxiliary axis mode in the next sampling time and retracts the electrode only along the auxiliary axis. The electrode does not move along the planned trajectory since the EDM machine's main controller receives gap voltage signal, which makes the machine's feed rate to zero after the feed rate override ($u_e=u_{eref}$).

2.2. Auxiliary axis mode ($M=1$)

The controller first checks P_{aux} to determine whether it has reached the position before the electrode retraction start. If $P_{aux}\geq P_F$ (the position of the auxiliary axis switches to the trajectory mode), the controller changes M–0, outputs u_{eref} to the EDM machine's main controller, and sets P_{com} to 0. The output runs the controller in trajectory mode in the next sampling time while maintaining the current electrode position along the trajectory and auxiliary axis. Setting P_F to a value smaller than the maximum physical position of the auxiliary axis, a smooth transitioning behavior between the auxiliary axis mode and trajectory mode is possible. If the position of the auxiliary axis was not checked before switching to trajectory mode, the machined surface would become wavy because it causes constant change in the depth of cut in the range of auxiliary axis motion.

If $P_{aux}<P_F$, the controller checks the difference between u_{eref} and u_e. If the voltage differential is positive, the controller maintains M–1, outputs u_{eref} to the EDM machine's main controller, and sets P_{com} as following:

$$P_{com}=K_F(u_{eref}-u_e), \tag{2}$$

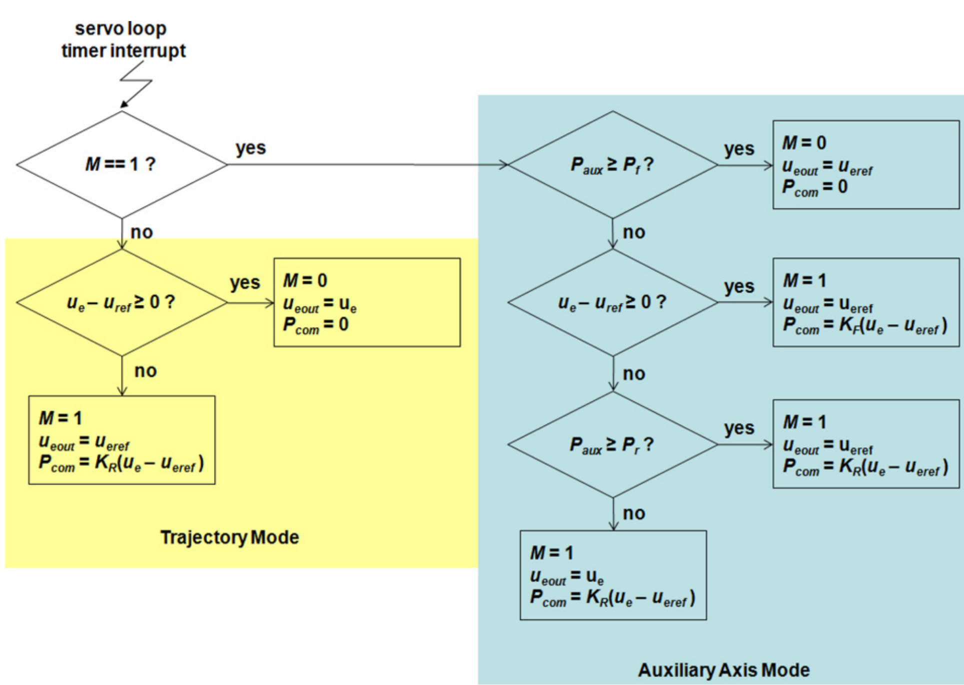

Fig. 3. Flowchart of proposed controller.

where K_F is the constant gain in proportional control for forwarding. The output runs the controller in auxiliary axis mode in the next sampling time and moves the electrode forward along the auxiliary axis while maintaining the electrode position along the trajectory.

If the voltage differential is negative, it checks the position of the electrode along the auxiliary axis. If $P_{aux} \geq P_R$ (the position of the auxiliary axis start retracting the electrode along the path), the controller maintains M at 1, outputs u_{eref} to the EDM machine's main controller, and sets P_{com} as in Eq. (1). The output runs the controller in auxiliary axis mode in the next sampling time and moves the electrode backward along the auxiliary axis while maintaining the electrode position along the trajectory.

If $P_{aux} < P_R$, the controller maintains M at 1, outputs u_e to the EDM machine's main controller, and sets P_{com} as in Eq. (1). The outputs run the controller in auxiliary axis mode in the next sampling time, then retracts the electrode along the auxiliary axis and trajectory. Because the MDR also exists at the inner trailing face of electrode, the electrode retracts along the trajectory, as shown in Fig. 1(d).

3. Experimental setup

As shown in Fig. 4, a die-sinking EDM machine (Model EDMS 150 H by EDM Solutions, Elk Grove Village, IL) is used as a base machine. A spindle system that can retract in high bandwidth is designed and fabricated to retract the electrode along its orientation direction. A piezo actuator (Model P-845.30 by Physik Instrumente GmbH, Karlsruhe, Germany) is used to retract the electrode with high bandwidth. To maximize the bandwidth, the load carried by the piezo actuator is minimized. Thrust bearings unit (Model 51101 by SKF, Göteborg, Sweden) and linear spline (Model LTR10AUUCL+50L-PK by THK, Tokyo, Japan) are used to transmit axial motion from the piezo actuator while allowing rotation. A DC motor (Model 82 830 009 by Crouzet, Coppell, Texas) connected by pulleys drives the linear spline to transmit rotational motion. An external controller board (Model ds1104 by dSPACE, Paderborn, Germany) is used to execute the proposed control algorithm. The spindle unit, external controller, and EDM machine's main controller (Model TNC 409 by Heidenhain, Traunreut, Germany) are wired as shown in the block diagram in Fig. 5(b). Unlike a conventional EDM controller shown in Fig. 5(a), the gap voltage is serially passed through the external controller to realize the proposed control strategy. In conventional EDM control, the machine movement is regulated by u_e, which provides information regarding the gap condition. The proposed control scheme replaces this u_e with u_{eout} as described earlier in Fig. 2. The proposed controller bypasses u_e from the machine, i.e., $u_{eout}=u_e$, in two situations. First, when sufficient gap condition is achieved without the need for auxiliary axis retraction, only the trajectory mode is activated. The other situation is when retraction in the trajectory direction is needed during the auxiliary mode operation. If the electrode is moved along the auxiliary axis, the position command to the auxiliary axis (P_{com}) is directly sent to the spindle, while u_{eout} is set based on the logic explained in Fig. 3. Other key output from the external controller is the analog position command. The position command is amplified by the piezo amplifier module (Model E-501 and E-505 by Physik Instrumente, Karlsruhe, Germany) to excite the piezo actuator. To suppress the structural vibration, a notch filter at 565 Hz and low pass filter with 500 Hz cutoff frequency are applied to the analog position command. Experimental verification yielded a step response of less than 2 ms with very small residual vibration at the spindle tip.

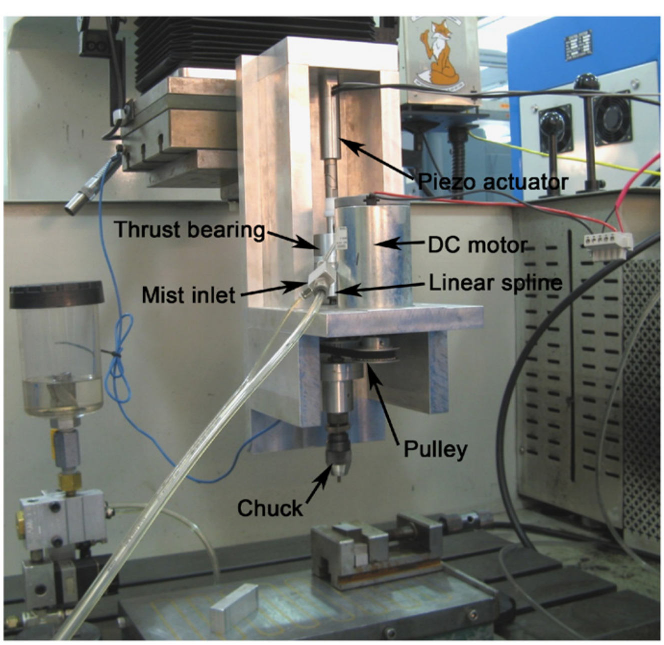

Fig. 4. Fabricated spindle and accelerometers mounted on spindle.

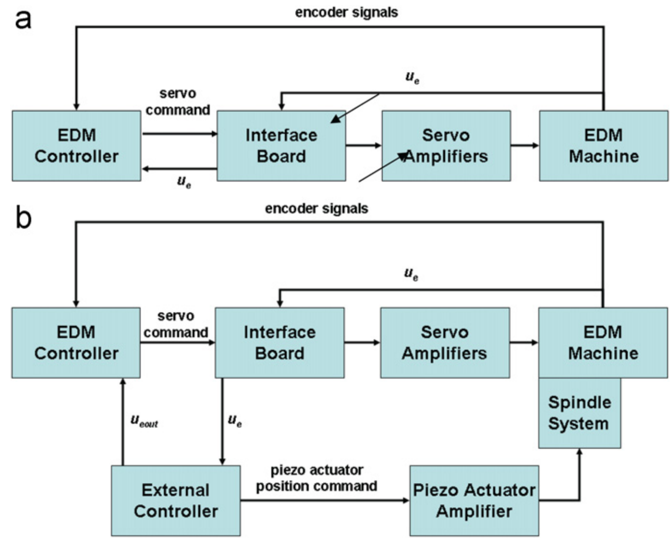

Fig. 5. System wiring diagram for (a) the conventional controller, and (b) the proposed controller.

Table 1 lists the discharge and control parameters for near-dry EDM milling with 5° lead angle, which is the electrode orientation with optimal MRR in the current near-dry EDM milling setup in roughing [25]. Since the discharge parameters used in the experiment are for roughing process, MRR and tool electrode wear ratio are the performance measure of interest. The lead angle is negative since the electrode is oriented away from the feed direction. The work-material is H13 tool steel, and the electrode is a copper tube. Electrode outer diameter is 3.2 mm, and electrode inner diameter, ϕ_{ID}, is 1.6 mm. Slots with 20 mm length and 0.5 mm depth are machined. Electrode rotational speed is set to 500 rpm. Compressed air at 517 kPa and kerosene liquid at 5 ml/min flow rate are supplied to the inlet.

The weight of the workpiece and electrode before and after the machining are measured using an Ohaus GA110 digital scale with 0.1 mg resolution to calculate the tool electrode wear ratio (η) and MRR. Based on the weight measurements, η and MRR are calculated as follows

$$\eta = \frac{\Delta m_{electrode}/\rho_{electrode}}{\Delta m_{workpiece}/\rho_{workpiece}} \quad (3)$$

Table 1
Discharge and control parameters for near-dry EDM milling experiment.

Discharge parameters	Value
Polarity	Negative
Open circuit voltage u_i (V)	200
Pulse duration t_i (μs)	4
Pulse interval t_o (μs)	8
Discharge current i_e (A)	20
Gap voltage u_e (V)	60
Control parameters	Value
Reference voltage ueref (V)	3
Forwarding constant KF	0.1
Retracting constant KR	0.5
Position to switch to trajectory mode PF	8
Position to start retracting along trajectory PR	7
Low pass filter cutoff frequency (Hz)	500
Notch filter frequency (Hz)	563

$$\mathrm{MRR} = \frac{\Delta m_{workpiece}/\rho_{workpiece}}{t} \quad (4)$$

where $\rho_{electrode}$ and $\Delta m_{electrode}$ are the density and mass change of electrode, respectively; $\rho_{workpiece}$ and $\Delta m_{workpiece}$ are the density and mass change of workpiece, respectively; and t is the machining time. In this study, $\rho_{workpiece}$ is 7800 kg/m^3 and $\rho_{electrode}$ is 8933 kg/m^3. A Taylor Hobson profilometer with 2 μm diamond stylus tip radius is used to measure the surface roughness along the slot. The arithmetical average roughness (R_a) is selected as the surface roughness parameter. The experiments with standard controller and proposed controller are repeated three times, and an analysis of variance (ANOVA) is carried out to investigate the statistical significance of the proposed controller.

4. Results and discussion

The performance of the proposed controller in terms of MRR, η, and R_a is compared with the conventional controller. Fig. 6(a)–(c) shows the experimental comparison of the proposed controller and conventional controller in MRR, η, and R_a, respectively. Bars represent the average value, while error bars represent the maximum and minimum value from the experiment. As shown in the figure, a 30% increase occurs in MRR while a small differences in η and R_a are observed. To interpret the results of the experiment, an analysis of variance (ANOVA) is carried out for MRR, η, and R_a. The results are summarized in Table 2. A 5% significance level was used as the criteria to determine whether the proposed controller has statistically significant effect; therefore, results with P-value smaller than 0.05 are statistically significant. The P-value for MRR, η, and R_a are 0.014, 0.439, and 0.551, respectively. Hence the controller improved the MRR by 30% without having statistically significant effect on η and R_a.

The improvement in the MRR of the proposed controller can be attributed to improved gap widening efficiency and use of high bandwidth piezo actuator for the auxiliary axis. Retracting the electrode in the axial direction for near-dry EDM milling with lead angle improves the gap widening efficiency. Fig. 7(a) and (b) shows a simplified drawing of electrode retraction for MDR 1 using the proposed and conventional controller, respectively. Geometry of tool electrode wear and electrode hole is omitted because they are more related to MDR 2. The proposed controller also retracts along the trajectory, which widens MDR 2 (same retraction direction as the conventional controller). Geometry that is related to MDR 2 can be omitted to compare and analyze the effect of electrode retraction. The actual gap widening for the conventional controller is $r_{act}=r\sin(\alpha)$, where r_{act} is the actual gap widening, r is the retraction distance by the electrode, and α is the lead angle. For the proposed controller, $r_{act}=r$, since the direction of electrode retraction is orthogonal to MDR 1. The efficiency of gap widening of conventional controller compared with proposed controller is equal to $\sin(\alpha)$ by taking a ratio of r_{act} from the conventional and proposed controller. Since $\alpha=5^\circ$ is used for this study, the conventional controller is only capable of widening 8.7% of the proposed gap controller assuming the same retraction distance. Having a high bandwidth piezo actuator also helped to improve the MRR. Auxiliary motion is much faster, and therefore, more efficient than the machine axis movement.

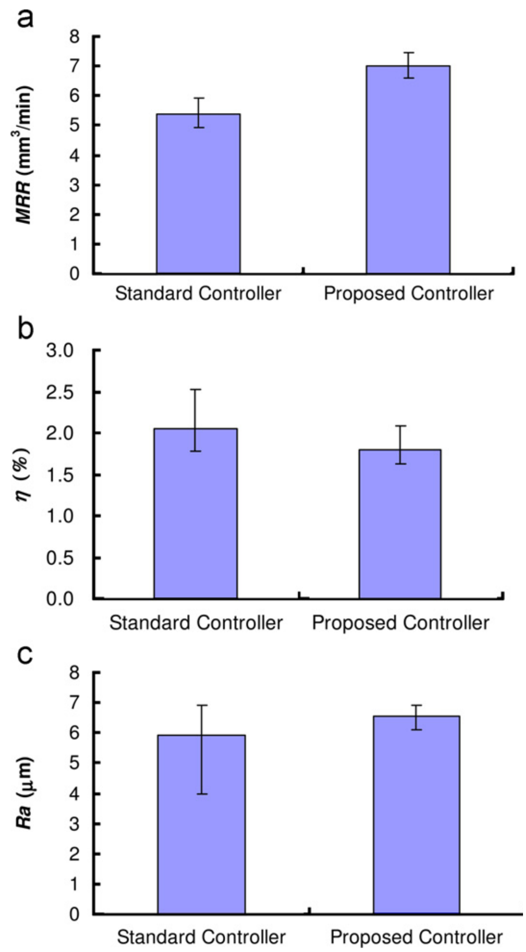

Fig. 6. Comparison of proposed controller and conventional controller (a) MRR, (b) η, and (c) R_a.

Table 2
ANOVA results of MRR, η, and R_a.

Source	DF	Seq SS	Adj SS	Adj MS	F	P
ANOVA results of MRR						
Method	1	3.8879	3.8879	3.8879	17.78	0.014
Error	4	0.8748	0.8748	0.2187		
Total	5	4.7616				
ANOVA results of η						
Method	1	0.0904	0.0904	0.0904	0.74	0.439
Error	4	0.4895	0.4895	0.1224		
Total	5	0.5798				
ANOVA results of R_a						
Method	1	0.611	0.611	0.611	0.42	0.551
Error	4	5.790	5.790	1.148		
Total	5	6.401				

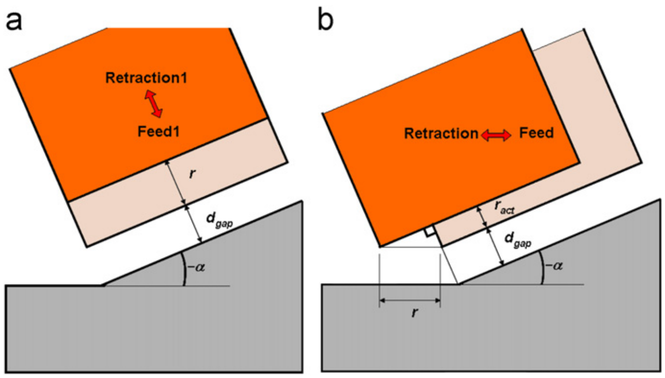

Fig. 7. Simplified schematic of gap widening efficiency for (a) proposed controller, and (b) conventional controller.

As defined in Eq. (3), η is related to the performance of a electrode material in removing the workpiece material. This is determined by the physics governed by thermoelectric behavior of the two materials in close proximity under high electrical potential. The fact that the proposed control scheme does not have statistically insignificant effect on η implies that the fundamental physics governing the material removal is not changed by adding a high bandwidth control. There is no reason to believe that the fundamental material removal mechanism should change by changing the electrode retracting direction and its frequency.

More efficiently enlarged gap improves the mist flow rate through MDR, which helps to maintain a good discharge gap condition by flushing debris. However, the change in gap distance is sensitive to the electrode motion along the electrode orientation. Therefore, the EDM performance is sensitive to the controller gains, the value of K_F and K_R. Fig. 8 shows the unstable performance of the proposed controller when inappropriate gains are selected. Fig. 8(a)–(c) shows the u_e from machine, u_{eout} sent to EDM controller, and total auxiliary axis position command, respectively, using too high controller gains of K_F=4 and K_R=8. The controller is unstable since the u_e and total auxiliary axis position command oscillates constantly, which results in continuous fluctuation of the gap distance. This constant oscillation of u_e and the auxiliary axis position are the result of arcing caused by high control gain, K_F. To avoid unstable discharges, the K_F must be reduced so the electrode does not move forward excessively to cause arcing, which may result in unfavorable outcome of low MRR, high η and high R_a. The other controller gain, K_R, could be increased to avoid unstable discharges since retracting the electrode enlarges the gap distance and decreases the chance of arcing. However, when K_R is too high, gap distance become too large and no discharge occurs, which results in low MRR. To tune the controller gains, the profile of u_e is monitored during discharge. The controller gains are adjusted to prevent the u_e from oscillating as in Fig. 8 and to maintain its value near 5 V. Prior experiments showed that u_e maintained at 5 V resulted in higher MRR and lower η, which is the sign of clean discharge gap with the proper gap distance.

Fig. 9 shows the operation of the proposed controller when appropriate gains are assigned. Fig. 9(a)–(c) shows u_e from machine, u_{eout} sent to EDM controller, and total auxiliary axis position command, respectively, using the tuned proposed controller with K_F=0.1 and K_R=0.5. Compared with u_e from the machine using the conventional controller, as shown in Fig. 9(d), u_e recovers faster when the proposed controller is used. Since u_e is directly related to the feed rate, faster recovery results in higher MRR. Conditions where the electrode retracted both in the trajectory and auxiliary directions were observed. While the auxiliary mode was in operation (see Fig. 9(c)), the u_{eout} fell below the u_{eref} of 3 V (Fig. 9(b)). This indicated that the electrode was retracting both in the trajectory and auxiliary directions. Also, note the small electrode retraction distance using the proposed controller (Fig. 9(c)). The piezo actuator only retracts one third of its motion range due to the efficient electrode retraction using the proposed controller algorithm.

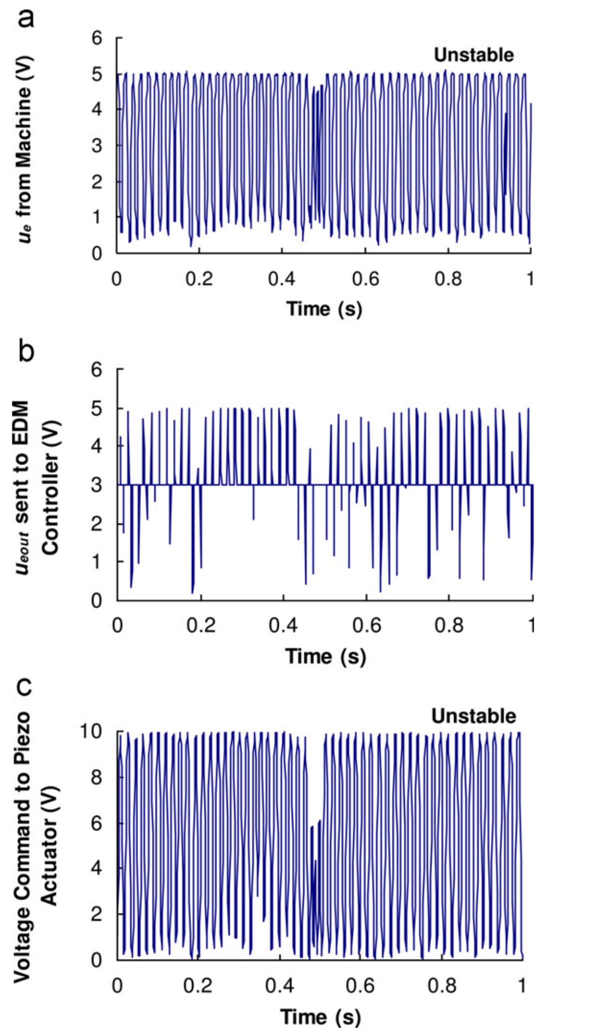

Fig. 8. Proposed controller with K_F=4 and K_R=8: (a) u_e from machine, (b) u_{eout} sent to EDM controller, and (c) total auxiliary axis position command.

5. Conclusions

A new gap control strategy for five-axis near-dry EDM milling was presented. The conventional EDM gap control method only retracts the electrode along the direction of command trajectrory. In five-axis EDM milling, this conventional strategy cannot effectively enlarge the gap distance because the orientation of the electrode and workpiece is not accounted for. A novel gap control system that can rapidly retract the electrode along its orientation in high bandwidth was designed and fabricated. A control structure that separated the electrode retraction and electrode feed along the path was developed and implemented. The new controller yielded 30% higher MRR without sacrificing η and surface roughness when compared with conventional controller. The new gap controller significantly improved the efficiency of electrode retraction on gap distance and increased the mist flow rate through MDR, which resulted in the MRR improvement.

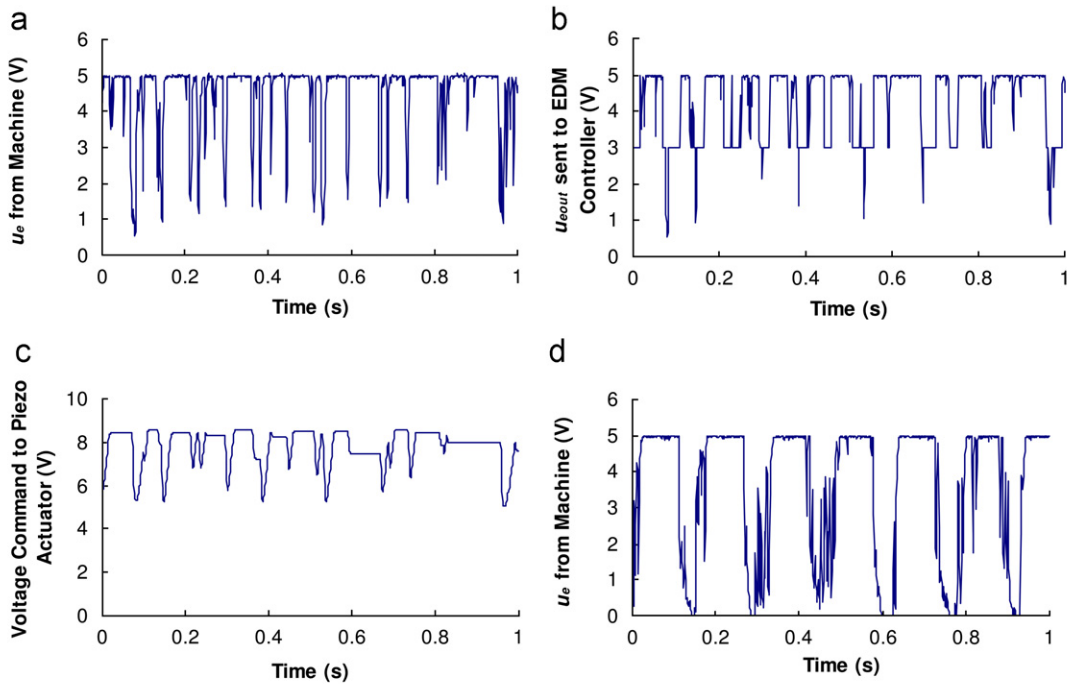

Fig. 9. Comparison of signals from the controller: proposed controller with K_F=0.1 and K_R=0.5 for (a) u_e from machine, (b) u_{eout} sent to EDM controller, and (c) total auxiliary axis position command; and (d) conventional controller for u_e from machine.

Current study utilizes simple feed rate override function and requires an external controller and special spindle. An integrated EDM control system can further improve the performance. In the future work, the internal controller within the EDM machine should be modified to control the discharge gap more effectively.

Acknowledgements

This research was sponsored by Advanced Technology Program, National Institute of Standards and Technology. The authors also appreciate supports from POM Group, Inc.

References

[1] M. Kunieda, B. Lauwers, K.P. Rajurkar, B.M. Schumacher, Advancing EDM through fundamental insight into the process, Annals of the CIRP 54 (2) (2005) 599–622.
[2] T. Kaneko, M. Tsuchiya, Three-dimensional numerically controlled contouring by electric discharge machining with compensation for the deformation of cylindrical tool electrodes, Precision Engineering 10 (3) (1988) 157–163.
[3] P. Bleys, J.P. Kruth, A. Zyrd, R. Delpretti, C. Tricarico, Real-time tool wear, Compensation in Milling EDM Annals of the CIRP 51 (1) (2002) 157–160.
[4] M. Kunieda, M. Yoshida, N. Taniguchi, Electrical discharge machining in gas, Annals of the CIRP 46 (1) (1997) 143–146.
[5] M. Kunieda, C. Furudate, High precision finish cutting by dry WEDM, Annals of the CIRP 50 (1) (2001) 121–124.
[6] M. Kunieda, Y. Miyoshi, T. Takaya, N. Nakajima, Z. Yu, M. Yoshida, High speed 3D milling by dry EDM, Annals of the CIRP 52 (1) (2003) 147–150.
[7] T. Wang, M. Kunieda, Dry WEDM for finish cut, Key Engineering Materials 259–260 (2004) 562–566.
[8] Z.B. Yu, J. Takahashi, M. Kunieda, Dry electrical discharge machining of cemented carbide, Journal of Materials Processing Technology 149 (2004) 353–357.
[9] Z.B. Yu, J. Takahashi, N. Nakajima, S. Sano, M. Kunieda, Feasibility of 3-D surface machining by dry EDM, International Journal of Electrical Machining 10 (2005) 15–20.
[10] J. Tao, A.J. Shih, J. Ni, Experimental study of the dry and near-dry electrical discharge milling processes, ASME Journal of Manufacturing Science and Engineering 130 (1) (2008) 011002-1-9.
[11] R. Snoeys, D. Dauw, M. Jennes, Survey of EDM adaptive control and detection systems, Annal of the CIRP 31 (2) (1982) 483–489.
[12] Y.F. Chang, VSS controller design for gap control of EDM, Japan Society of Mechanical Engineering, International Journal, Series C 45 (3) (2002) 712–721.
[13] J.H. Zhang, H. Zhang, D.S. Su, Y. Qin, M.Y. Huo, Q.H. Zhang, L. Wang, Adaptive fuzzy control system of a servomechanism for electro-discharge machining combined with ultrasonic vibration, Journal of Materials Processing Technology 129 (1–3) (2002) 45–49.
[14] C.C. Kao, A.J. Shih, S.F. Miller, Fuzzy logic control of micro-hole electrical discharge machining, ASME Journal of Manufacturing Science and Engineering 130 (2008) 064502-1-6.
[15] C.C. Kao, A.J. Shih, Design and tuning of the adaptive fuzzy logic controller for micro-hole electrical discharge machining, Journal of Manufacturing Processes 10 (1) (2008) 61–73.
[16] K.H. Ho, S.T. Newman, State of the art electrical discharge machining (EDM), International Journal of Machine Tools and Manufacture 43 (13) (2003) 1287–1300.
[17] V.S.R. Murthy, P.K. Philip, Pulse train analysis in ultrasonic assisted EDM, International Journal of Machine Tools and Manufacture 27 (4) (1987) 447–469.
[18] D. Kremer, L. Lebrun, A. Moisan, Effects of ultrasonic vibrations on the performance in EDM, Annals of the CIRP 38 (1) (1989) 199–202.
[19] D. Kremer, C. Lhiaubet, A. Moisan, A study of the effect of synchronizing ultrasonic vibrations with pulses in EDM, Annals of the CIRP 40 (1) (1991) 211–214.
[20] S. Enache, C. Opran, G. Stoica, The study of EDM with forced vibration of tool-electrode, Annals of the CIRP 39 (1) (1990) 167–170.
[21] J.H. Zhang, T.C. Lee, W.S. Lau, X. Ai, Spark erosion with ultrasonic frequency, Journal of Materials Processing Technology 68 (1) (1997) 83–88.
[22] J.H. Zhang, H. Zhang, D.S. Su, Y. Qin, M.Y. Huo, Q.H. Zhang, L. Wang, Adaptive fuzzy control system of a servomechanism for electro-discharge machining combined with ultrasonic vibration, Journal of Materials Processing Technology 129 (1-3) (2002) 45–49.
[23] Q.H. Zhang, R. Du, J.H. Zhang, Q.B. Zhan, An investigation of ultrasonic-assisted electrical discharge machining in gas, International Journal of Machine Tools and Manufacture 46 (12–13) (2006) 1582–1588.
[24] Q.H. Zhang, J.H. Zhang, Q.B. Zhang, S.P. Su, Experimental research on technology of ultrasonic vibration aided electrical discharge machining (UEDM) in gas, Key Engineering Materials 315–316 (2006) 81–84.
[25] M. Fujiki, J. Ni, A.J. Shih, Investigation of the effect of electrode orientation and fluid flow in near-dry EDM milling, International Journal of Machine Tools and Manufacture 49 (10) (2009) 749–758.
[26] Y. Imai, A. Satake, A. Taneda, K. Kobayashi, Improvement of EDM machining speed by using high frequency resonse actuator, International Journal of Electrical machining 1 (1996) 21–26.
[27] Y. Imai, T. Nakagawa, H. Miyake, H. Hidai, H. Tokura, Local actuator module for highly accurate micro-EDM, Journal of Materials Processing Technology 149 (1–3) (2004) 328–333.
[28] I. Beltrami, C. Joseph, R. Clavel, J.P. Bacher, S. Bottinelli, Micro- and nanoelectric-discharge machining, Journal of Materials Processing Technology 149 (1–3) (2004) 263–265.
[29] M. Kunieda, T. Takaya, S. Nakano, Improvement of dry EDM characteristics using piezoelectric actuator, Annals of the CIRP 53 (1) (2004) 183–186.